Wave Motion 89 (2019) 221–231

Contents lists available at ScienceDirect

Wave Motion

journal homepage: www.elsevier.com/locate/wamot

Coupled-mode theory for stationary and nonstationary resonant sound propagation

Theodoros T. Koutserimpas, Romain Fleury *

Laboratory of Wave Engineering, École Polytechnique Fédérale de Lausanne (EPFL), 1015 Lausanne, Switzerland

HIGHLIGHTS

- Coupled-mode equations for stationary and nonstationary resonant sound systems.
- Hamiltonian method approach for couple-mode theory parameters.
- Perturbation analysis applied to the Hamiltonian of a nonstationary wave system.
- Examples presented for stationary and nonstationary sound resonant problems.

ARTICLE INFO

Article history:
Received 27 November 2018
Received in revised form 29 January 2019
Accepted 24 March 2019
Available online 28 March 2019

Keywords:
Coupled-mode theory
Hamiltonian analysis
Resonant sound propagation
Perturbation analysis
Stationary and nonstationary dynamics

ABSTRACT

In this paper, we present a complete analytical derivation of the equations used for stationary and nonstationary wave systems regarding resonant sound transmission and reflection described by the phenomenological coupled-mode theory. We calculate the propagating and coupling parameters used in coupled-mode theory directly by utilizing the generalized eigenwave-eigenvalue problem from the Hamiltonian of the sound wave equations for the problem of a one-dimensional isolated on-channel resonance. This Hamiltonian formalization could be beneficial and could potentially model and parameterize a broad range of acoustic wave phenomena. We demonstrate how to use this theory as a basis for perturbation analysis of complex resonant scattering scenarios. In particular, we form the effective Hamiltonian and coupled-mode parameters for the study of sound resonators with background moving media. Finally, we provide a comparison between coupled-mode theory and full-wave numerical examples, which validate the Hamiltonian approach as a relevant model to compute the scattering characteristics of waves by complex resonant systems.

1. Introduction

Wave manipulation and control by resonant media has been on the frontline of wave engineering research in the past decades. Research in wave physics and related technologies has illustrated extreme wave propagation and scattering properties, which enrich the theory of waves, vibrations and involuntary oscillations, and can be applied to a broad spectrum of potential applications and technologies. From metamaterials and metasurfaces to photonic and phononic crystal devices, resonators have attested to play a crucial role imparting unique wave propagation properties and effective parameters. One of the mathematical methods to model wave propagation in resonant media is coupled-mode theory (CMT). CMT is a mathematical abstract tool employed to formulate the energy transitions of coupled-resonant

* Correspondence to: EPFL STI IEL LWE ELB 030 Station 11, CH-1015, Lausanne, Switzerland.
E-mail address: romain.fleury@epfl.ch (R. Fleury).

https://doi.org/10.1016/j.wavemoti.2019.03.011

systems. CMT is mainly used to predict traveling waves or oscillating states in classical and quantum mechanics, electromagnetics and acoustics [1–11]. More specifically, it has been used to describe wave propagation properties in stationary, nonstationary, linear and nonlinear resonances [1,12–16]. Due to its minimalism, the resulting equations of CMT attract a lot of attention and usage by researchers. While the simplicity of such method is undeniable, the parameters used are most often a product of intuition of the examined physical system or a result of experimental or numerical fitting procedures. In this research paper, we consider the case of resonant sound wave transmission and reflection and we provide the exact analytical coupled-mode-theory parameters without presuming specific wave conditions or implementing numerical fitting techniques. This is achieved by formulating a Schrödinger type matrix formalization of the acoustic wave equations regarding the sound pressure and the particle velocity. The advantage of this approach is that it can be utilized as an orthogonal basis for the perturbation analysis of more peculiar resonant scattering systems. To evidence this we consider the example of resonant sound transmission and reflection in nonstationary systems, i.e. acoustic resonators subject to the motion of the acoustic background medium. The CMT analysis and the results are in total agreement with the full-wave simulations, which applied the finite element method (FEM) [17].

2. The generalized eigenvalue problem: From sound waves to Schrödinger formalization

The equations regarding linear acoustical wave propagation in a lossless homogeneous medium can take the simple form of

$$\nabla \vec{u} = -\frac{1}{K_0}\partial_t p, \tag{1}$$

$$\nabla p = -\rho_0 \partial_t \vec{u}, \tag{2}$$

where ρ_0 is the density, K_0 is the bulk modulus of the medium and $\vec{u}$, p are the particle velocity and the sound pressure, respectively. Note that $c = \sqrt{K_0/\rho_0}$ where c is the velocity of the acoustic wave in the medium. The density and the bulk modulus can be space dependent ($K_0 = K_0(\vec{r})$, and $\rho_0 = \rho_0(\vec{r})$). Eqs. (1) and (2) can form a Schrödinger system with the appropriate mathematical manipulation of the equations. For this purpose, the sound state function (ket) could be expressed as:

$$|\Psi\rangle = \begin{pmatrix} p \\ \vec{u} \end{pmatrix}. \tag{3}$$

The inner product of these vectors is defined as $\langle \Psi_a | \Psi_b \rangle = \iiint \left(p_a^* p_b + \vec{u}_a^* \cdot \vec{u}_b \right) dV$. We also designate a weighting operator related to the acoustical properties of the medium

$$\hat{\zeta} = \begin{pmatrix} \frac{1}{K_0} & 0 \\ 0 & \rho_0 \mathbf{I}_{3\times 3} \end{pmatrix}. \tag{4}$$

In general $\hat{\zeta}$ can define any type of medium (isotropic, anisotropic and bianisotropic [18,19]), however here we focus on the simple case of a homogeneous fluid. Notice that the assumption of lossless medium results in a Hermitian weighting operator ($\hat{\zeta} = \hat{\zeta}^\dagger$). The Hamiltonian of the system is given by

$$\mathcal{H} = -j \begin{pmatrix} 0 & \nabla\cdot \\ \nabla & 0 \end{pmatrix}. \tag{5}$$

The Hamiltonian is Hermitian if and only if $\langle \Psi_a | \mathcal{H} \Psi_b \rangle = \langle \mathcal{H} \Psi_a | \Psi_b \rangle$ for two arbitrary solutions of the same boundary-condition problem. It can be proven that the Hamiltonian is indeed Hermitian when the system is made of finite localized resonances and the wave energy is conserved (the incident and scattered fields produce to a sum of integrals which result to zero for $r \to \infty$). Another case where the operator is Hermitian is for lossless structures, which possess space periodicity, and the sound state functions have to obey the Bloch theorem [20]. This implies that it is also Hermitian for any isolated two-port system, since one can always take periodic boundary conditions at infinity. Finally, from Eqs. (3)–(5), the resulting Schrödinger system is

$$j\hat{\zeta} \cdot \partial_t |\Psi\rangle = \mathcal{H} |\Psi\rangle. \tag{6}$$

If one considers the case of time-harmonic fields the problem is simplified. The sound state function becomes $|\Psi(\vec{r}, t)\rangle = |\psi(\vec{r}, t)\rangle e^{-j\omega t}$, and the Schrödinger equation (6) is of the form

$$\omega_m \hat{\zeta} |\psi_m\rangle = \mathcal{H} |\psi_m\rangle. \tag{7}$$

For Hermitian matrices $\mathcal{H}$ and $\hat{\zeta}$ the resonant frequencies ω_m are real, and their set is continuous or discrete depending on the under examined problem. Different eigenfrequencies $\omega_m \neq \omega_n$ correspond to eigenwaves $|\psi_m\rangle, |\psi_n\rangle$ which are orthogonal. Hence, they satisfy the orthogonality condition:

$$\langle \psi_n | \hat{\zeta} \psi_m \rangle = 0. \tag{8}$$

Additionally, in such Hermitian systems the existence of a solution $|\psi_m\rangle$ with positive (or negative) frequency leads to the formulation of an extra independent solution $\left|\hat{\sigma}_z\psi_m\right\rangle$ with negative (or positive) frequency, i.e.:

$$-\omega_m\hat{\zeta}\left|\hat{\sigma}_z\psi_m\right\rangle = \mathcal{H}\left|\hat{\sigma}_z\psi_m\right\rangle, \tag{9}$$

where $\hat{\sigma}_z$ is the third order Pauli matrix [20]. In order to return the solution of Eq. (9) to the same frequency with Eq. (7) we can simply apply the complex conjugation operator. By doing so, we obtain that the system has two independent solutions at the same frequency. A physical interpretation of the relation of Eq. (9) is that in any homogeneous reciprocal medium, a duality of wave solutions with opposite propagating direction is always found.

$$\left|\psi_m^+\right\rangle = \begin{pmatrix} p_m \\ \vec{u}_m \end{pmatrix}, \quad \left|\psi_m^-\right\rangle = \begin{pmatrix} p_m^* \\ -\vec{u}_m^* \end{pmatrix}. \tag{10}$$

Taking this into account, the orthogonality relation (8) has to hold also for the forward and backward propagating modes:

$$\left\langle \psi_n \middle| \hat{\zeta}\hat{\sigma}_z\psi_m \right\rangle = 0. \tag{11}$$

Eq. (11) is of great physical importance. Further to the obvious orthogonality that it implies, it also proves that for the same mode ($m = n$) the potential energy of the wave mode which is stored in the acoustic pressure is the same with the kinetic energy stored in the motion of the medium's particles $\left(\iiint \frac{1}{K_0}|p_m|^2\,dV = \iiint \rho_0\left|\vec{u}_m\right|^2 dV\right)$. Finally, note that all these considerations are true not only in three-dimensions (3D), but also for 2D and 1D, for which the only changes are that three-dimensional integrals reduce to 2D and 1D ones.

3. Eigenwave bases and scattering analysis

3.1. Traveling wave basis

We assume a traveling wave basis for the solution of the wave distribution at some frequency near a resonant frequency ω_m. This wave formulation is the following

$$|\Psi\rangle = \alpha_+(\vec{r},t)\left|\psi_m^+\right\rangle e^{-j\omega_m t} + \alpha_-(\vec{r},t)\left|\psi_m^-\right\rangle e^{-j\omega_m t}. \tag{12}$$

To proceed further to the coupled-mode analysis, we need to make important approximations in Eq. (12) about the variations of the envelopes of the waves in positive and negative direction, α_+ and α_-. As advocated by a general assumption of weak coupling (see for instance [2]) these envelopes are presumed to be slowly varying in space and time. Plugging (12) into (6) gives the following equation

$$j\hat{\zeta}\left(\partial_t\alpha_+\left|\psi_m^+\right\rangle + \partial_t\alpha_-\left|\psi_m^-\right\rangle\right) = \mathcal{H}(\alpha_+)\left|\psi_m^+\right\rangle + \mathcal{H}(\alpha_-)\left|\psi_m^-\right\rangle, \tag{13}$$

where $\mathcal{H}(\alpha_\pm)$ is the Hamiltonian operating just on the envelopes $\alpha_\pm$. Eq. (13) provides the fundamental relation of CMT. It is possible to form CMT by projecting the bras $\left\langle\psi_m^\pm\right|$ to Eq. (13). The resulting terms from these projections are:

$$\left\langle \psi_m^- \middle| \hat{\zeta}\psi_m^+ \right\rangle = 2\iiint \frac{1}{K_0}p_m^2 dV \tag{14}$$

$$\left\langle \psi_m^+ \middle| \hat{\zeta}\psi_m^- \right\rangle = 2\iiint \frac{1}{K_0}\left(p_m^*\right)^2 dV \tag{15}$$

$$\left\langle \psi_m^\pm \middle| \hat{\zeta}\psi_m^\pm \right\rangle = 2\iiint \frac{1}{K_0}|p_m|^2 dV \tag{16}$$

and the system's overall directional energy flux is

$$\vec{\mathcal{F}}_e = \iiint \mathrm{Re}\left\{p_m^*\vec{u}_m\right\} dV, \tag{17}$$

The two final equations from the projections are

$$\partial_t\alpha_+ + (\vec{v}_g\nabla)\alpha_+ = -g^*\partial_t\alpha_-, \tag{18}$$
$$\partial_t\alpha_- - (\vec{v}_g\nabla)\alpha_- = -g\partial_t\alpha_+, \tag{19}$$

where $g = \frac{\left\langle\psi_m^-\middle|\hat{\zeta}\psi_m^+\right\rangle}{\left\langle\psi_m^\pm\middle|\hat{\zeta}\psi_m^\pm\right\rangle}$, and $\vec{v}_g = \frac{2\vec{\mathcal{F}}_e}{\left\langle\psi_m^\pm\middle|\hat{\zeta}\psi_m^\pm\right\rangle}$. By the observation of Eqs. (18) and (19), some interesting features could be extracted and explained. For example, the parameter g can characterize the homogeneity of the medium and the localization of the field in the resonators. If the chosen medium has no defects or cavities $\left\langle\psi_m^-\middle|\hat{\zeta}\psi_m^+\right\rangle \approx 0$, and in consequence $g \approx 0$, which means that there is no coupling between the two envelopes α_+, α_-. But if a defect is placed the wave propagation problem supports a back scattered mode and the total field is localized. In this case $g \neq 0$. Of course, the absolute value of g has an upper bound for any case of wave propagation, due to the way it is normalized ($|g| \leq 1$). Taking a closer look at $\vec{v}_g$, we find that aside from the normalization, it is proportional to the vector $\vec{S} = \text{Re}\left\{p_m \vec{u}_m^*\right\}$, which describes the acoustic power flow. This directional flux satisfies the solenoidal field condition: $\nabla\vec{S} = 0$ in steady state and in the absence of active elements, due to the general continuity equation. The resulting algebra for the computation of $\vec{v}_g$ provides a quantitative parameter that characterizes the effective group velocity of the wave. An additional remark is that the inverse norm, i.e. $1/\left|\vec{v}_g\right|$ is proportional to the decay rate of the resonator. All these quantities can be computed from the knowledge of the mode profiles p_m and $\vec{u}_m$ of the linear problem.

3.2. Standing wave basis

Instead of applying the traveling waves $\left|\psi_m^+\right\rangle, \left|\psi_m^-\right\rangle$ as basis of the solution, it is possible to define standing waves $\left|\psi_A\right\rangle, \left|\psi_B\right\rangle$ which, depending on the under examined problem, could provide a more practical mathematical formulation when used as basis of the wave solution of parity antisymmetric or symmetric structures. The even ($\left|\psi_A\right\rangle$) and odd ($\left|\psi_B\right\rangle$) modes are defined as

$$\left|\psi_A\right\rangle = \frac{\left|\psi_m^+\right\rangle + \left|\psi_m^-\right\rangle}{2} = \begin{pmatrix} \text{Re}\left\{p_m\right\} \\ j\text{Im}\left\{\vec{u}_m\right\} \end{pmatrix}, \tag{20}$$

$$\left|\psi_B\right\rangle = \frac{\left|\psi_m^+\right\rangle - \left|\psi_m^-\right\rangle}{2j} = \begin{pmatrix} \text{Im}\left\{p_m\right\} \\ -j\text{Re}\left\{\vec{u}_m\right\} \end{pmatrix}, \tag{21}$$

These modes represent even and odd standing waves. The $\vec{S}$ vector is zero separately for both $\left|\psi_A\right\rangle, \left|\psi_B\right\rangle$. The traveling waves can be constructed from the odd and even standing basis: $\left|\psi_m^\pm\right\rangle = \left|\psi_A\right\rangle \pm j\left|\psi_B\right\rangle$. In the case of choosing the standing wave basis, we assume wave solutions of the form

$$\left|\Psi\right\rangle = A(\vec{r}, t)\left|\psi_A\right\rangle e^{-j\omega_m t} + jB(\vec{r}, t)\left|\psi_B\right\rangle e^{-j\omega_m t}. \tag{22}$$

Plugging Equation (22) into (6) gives us a general equation

$$j\hat{\zeta}\left(\partial_t A\left|\psi_A\right\rangle + j\partial_t B\left|\psi_B\right\rangle\right) = \mathcal{H}(A)\left|\psi_A\right\rangle + j\mathcal{H}(B)\left|\psi_B\right\rangle. \tag{23}$$

Following the same mathematical procedure as before we form the projections of both bras (even and odd sound state functions) to Eq. (23). This results to two equations, which follow

$$(1+g)\,\partial_t A + \left(\vec{v}_g \nabla\right) B = 0, \tag{24}$$

$$(1-g)\,\partial_t B + \left(\vec{v}_g \nabla\right) A = 0, \tag{25}$$

where $g, \vec{v}_g$ are defined in Section 2. This formulation based on even and odd modes can be very useful when dealing with mirror symmetric structures and antisymmetric acoustic crystals. In such structures, it is common that either the odd or the even mode dominate, depending on the operating frequency. It is straightforward to show that $g = \frac{\iiint (1/K_0)\left[p_A^2 - p_B^2\right] dV}{\iiint (1/K_0)\left[p_A^2 + p_B^2\right] dV}$. In the case that the even mode dominates $g \to 1$ and the system of equations is significantly simplified. In a close analogy, when the odd mode dominates when $g \to -1$ and a similar simplification of the field can be implemented.

3.3. Scattering analysis

Let us assume a one-dimensional structure from $x = 0$ to $x = L$ as depicted in Fig. 1, which forms an on-channel resonance system. The notations u_+ and v_+ are used to symbolize the incoming signals on the left and the right side and u_-, v_- the outgoing signals on the left and the right side, respectively. The scattering analysis comes down to the specification of the scattering matrix, i.e. the matrix S_0, which connects the outgoing with the incoming wave signals

$$\begin{pmatrix} u_- \\ v_- \end{pmatrix} = S_0 \begin{pmatrix} u_+ \\ v_+ \end{pmatrix}, \tag{26}$$

$$S_0 = \begin{pmatrix} r_L & t \\ t & r_R \end{pmatrix}, \tag{27}$$

where r_L, r_R are the reflection coefficients from the right and the left side and t is the transmission coefficient at a normal incidence. Utilizing the analysis based on the traveling waves and approximating the wave distributions with averages we get: $\alpha_\pm \approx \left(u_\pm + v_\mp\right)/2$. Using finite difference approximations (which are valid approximations for weak

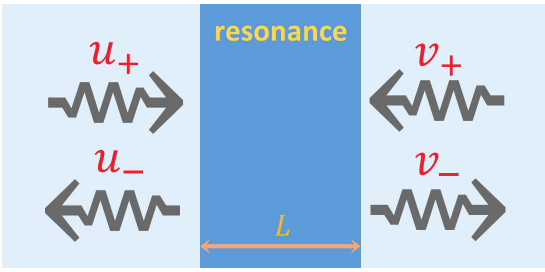

Fig. 1. Schematic representation of a one-dimensional sound resonant system with input and output wave signals from the left and right directions.

coupling problems or strong inhomogeneities with considerably small length [2]), we write: $\partial_x \alpha_\pm \approx (v_\mp - u_\pm)/L$ and $\partial_t \alpha_\pm \approx -j(\omega - \omega_m)(u_\pm + v_\mp)/2$, where ω_m is the resonant frequency and ω is the incident field frequency. The mathematical model assumes an average of the wave distributions, where the mode traveling in the positive direction is the average of the signal that enters from the left and the signal that leaves the structure from the right direction. In analogous way, the traveling mode at the negative direction is the average of the signal that enters from the right and leaves from the left. Additionally, the space derivative is modeled as a first order approximation. These assumptions are valid under weak coupling approximation, which assumes that the energy of the mode decays exponentially, and is true for large quality factors $Q \gg 1$. By plugging these expressions into (18), (19), the scattering matrix becomes:

$$S_0 = \frac{1}{1 - \frac{j(\omega - \omega_m)}{\gamma}} \begin{pmatrix} \frac{jg(\omega-\omega_m)}{\gamma} & 1 \\ 1 & \frac{jg*(\omega-\omega_m)}{\gamma} \end{pmatrix}, \tag{28}$$

where $\gamma = \vec{v}_g \cdot \vec{n}/L$ is the (radiative) decay rate and $\vec{n}$ is the unit vector in the direction of the wave propagation. From Eq. (28) it is clear that the transmission and backscattering shape-lines are Lorentzian, as expected for resonant systems. Using the standing wave basis, we get the same results:

$$\frac{1+g}{2} d_t A = -\gamma A + \gamma(u_+ + v_+), \tag{29}$$

$$\frac{1-g}{2} d_t B = -\gamma B + \gamma(u_+ - v_+). \tag{30}$$

For a dominant even mode ($g \to 1$) the scattering analysis is

$$d_t A = -\gamma A + \gamma(u_+ + v_+) \tag{31}$$

$$\begin{pmatrix} u_- \\ v_- \end{pmatrix} = -\begin{pmatrix} u_+ \\ v_+ \end{pmatrix} + A \begin{pmatrix} 1 \\ 1 \end{pmatrix} \tag{32}$$

For a dominant odd mode ($g \to -1$) the scattering analysis is

$$d_t B = -\gamma B + \gamma(u_+ - v_+) \tag{33}$$

$$\begin{pmatrix} u_- \\ v_- \end{pmatrix} = \begin{pmatrix} u_+ \\ v_+ \end{pmatrix} + B \begin{pmatrix} -1 \\ 1 \end{pmatrix}. \tag{34}$$

At resonance, the dominant even mode has a transmission coefficient of 1, whereas at resonance the dominant odd mode the transmission coefficient is -1. Notice that the under examined problem can include multiple resonators, and in consequence the generalized eigenvalue problem as described above finds the overall resonance frequencies and eigenwaves of the total system and there is no need to find numerical fits for the inner coupling coefficients of the resonators.

4. Sound resonance in a background moving medium

4.1. Perturbation method

In sound wave engineering, the mathematical modeling of wave propagation in nonstationary media is of great importance, in a variety of applications such as noise detection, imaging and Doppler-based devices [21,22]. In these specific cases, the Galilean principle of relativity [23] is applied and only the longitudinal material disturbance upsets the propagating waves. We consider a material disturbance such that it can be modeled as a background material movement of a velocity of $\vec{w}_{\rm b}$. The sound wave differential equations are [24]:

$$(\partial_t + \vec{w}_{\rm b} \cdot \nabla)\, p + K_0 \nabla \vec{u} = 0 \tag{35}$$

$$(\partial_t + \vec{w}_{\rm b} \cdot \nabla)\, \vec{u} + \left(\vec{u} \cdot \nabla\right) \vec{w}_{\rm b} + \nabla p/\rho_0 = 0 \tag{36}$$

In order to form the CMT of such systems we apply a perturbative method, assuming the added extra terms, which describe the perturbative effects are weak. The effective Hamiltonian of the acoustic system is now:

$$j\hat{\zeta} \cdot \partial_t \left|\Psi\right\rangle = \mathcal{H}_{\rm eff} \left|\Psi\right\rangle , \tag{37}$$

$$\mathcal{H}_{\rm eff} = \mathcal{H} + \Delta\mathcal{H}_{\rm b}, \tag{38}$$

where $\mathcal{H}$ is the Hamiltonian as defined in Eq. (5) of the stationary system and $\Delta\mathcal{H}_{\rm b}$ corresponds to the extra terms added at the wave Eqs. (35), (36) due to the nonstationary dynamics of the medium. As a side note, we stress that the Hamiltonian resulting from the perturbation analysis $\mathcal{H}_{\rm eff}$ does not have to be Hermitian, and could be used to include the perturbative effects of losses, time-varying medium properties, or nonlinearities etc. (the focus of the present analysis is, however on a simplified nonstationary problem). Following the same mathematical analysis as before, we derive:

$$\Delta\mathcal{H}_{\rm b} = -j \begin{pmatrix} \frac{1}{K_0}\left(\vec{w}_{\rm b} \cdot \nabla\right) & 0 \\ 0 & \rho_0 \left((\vec{w}_{\rm b} \cdot \nabla) + \mathcal{D}\vec{w}_{\rm b}\right) \end{pmatrix}, \tag{39}$$

where:

$$\mathcal{D}\vec{w}_{\rm b} = \begin{pmatrix} \partial_x w_{\rm bx} & 0 & 0 \\ 0 & \partial_y w_{\rm by} & 0 \\ 0 & 0 & \partial_z w_{\rm bz} \end{pmatrix}. \tag{40}$$

Assuming traveling wave basis, we form the generalized eigenvalue problem from the general equation:

$$j\hat{\zeta}\left(\partial_t \alpha_+ \left|\psi_m^+\right\rangle + \partial_t \alpha_- \left|\psi_m^-\right\rangle\right) = \mathcal{H}(\alpha_+)\left|\psi_m^+\right\rangle + \Delta\mathcal{H}_{\rm b}(\alpha_+)\left|\psi_m^+\right\rangle + \mathcal{H}(\alpha_-)\left|\psi_m^-\right\rangle + \Delta\mathcal{H}_{\rm b}(\alpha_-)\left|\psi_m^-\right\rangle. \tag{41}$$

Following the same analysis and projecting Eq. (40) with $\left\langle\psi_m^\pm\right|$ we get the perturbed CMT equations:

$$\partial_t \alpha_+ + (\vec{v}_{g_{\rm eff}}^{\,+} \nabla)\alpha_+ + m_{\rm b}\alpha_+ = -g^* \partial_t \alpha_- - (\vec{\theta}_{\rm b}^{\,*} \nabla)\alpha_- - \kappa_{\rm b}^* \alpha_-, \tag{42}$$

$$\partial_t \alpha_- - (\vec{v}_{g_{\rm eff}}^{\,-} \nabla)\alpha_- + m_{\rm b}\alpha_- = -g \partial_t \alpha_+ - (\vec{\theta}_{\rm b} \nabla)\alpha_+ - \kappa_{\rm b}\alpha_+, \tag{43}$$

where the extra nonstationary coefficients are obtained from the stationary modes as:

$$\vec{v}_{g_{\rm eff}}^{\,\pm} = \vec{v}_g \pm 2 \iiint \vec{w}_{\rm b} \left(\frac{|p_m|^2}{K_0}\right) dV \Big/ \left\langle \psi_m^\pm \middle| \hat{\zeta}\, \psi_m^\pm \right\rangle = \vec{v}_g \pm \Delta\vec{v}_{\rm b}, \tag{44}$$

$$m_{\rm b} = \iiint \partial_{\vec{n}} \vec{w}_{\rm b} \left(\rho_0 \left|\vec{u}_m\right|^2\right) dV \Big/ \left\langle \psi_m^\pm \middle| \hat{\zeta}\, \psi_m^\pm \right\rangle, \tag{45}$$

$$\vec{\theta}_{\rm b} = 2 \iiint \vec{w}_{\rm b} \left(\frac{p_m^2}{K_0}\right) dV \Big/ \left\langle \psi_m^\pm \middle| \hat{\zeta}\, \psi_m^\pm \right\rangle, \tag{46}$$

$$\kappa_{\rm b} = \iiint \partial_{\vec{n}} \vec{w}_{\rm b} \left(\rho_0 \vec{u}_m^2\right) dV \Big/ \left\langle \psi_m^\pm \middle| \hat{\zeta}\, \psi_m^\pm \right\rangle. \tag{47}$$

Evidently, the coefficients $\vec{v}_{g_{\rm eff}}^{\,\pm}$ and $\vec{\theta}_{\rm b}$ correspond to the scattering effects of the nonstationary operative normalized group velocity, for wave propagation at the same $(+)$ and opposite $(-)$ direction of the disturbance $\vec{w}_{\rm b}$. In addition, $m_{\rm b}$ and $\kappa_{\rm b}$ are normalized coefficients which represent the dynamical influence of an attenuated or an accelerated active nonstationary background medium (at the direction of the wave propagation $\vec{n}$).

4.2. Eigenfrequencies of sound resonances with background movement

Let us assume a simple one-dimensional problem, in which the sound wave has particle velocity $\vec{u} = [u_x, 0, 0]^{\mathrm{T}}$ and scalar sound pressure p and there is no dependence on the other coordinates ($\partial_y = \partial_z = 0$). Before applying CMT to this system, let us analyze it using a direct method in order to extract its main scattering properties. Taking into account the general differential Eqs. (35), (36) which describe sound waves in background moving wave media we assume phasors for the scalar pressure p and the particle velocity vector $\vec{u}$. Furthermore, we assume $\vec{w}_{\mathrm{b}} = [w_{\mathrm{bx}}, 0, 0]^{\mathrm{T}}$ without degenerating the wave solution. The two modified equations are:

$$j\omega p + w_{\mathrm{bx}} d_x p + K_0 d_x u_x = 0, \tag{48}$$

$$j\omega u_x + w_{\mathrm{bx}} d_x u_x + u_x d_x w_{\mathrm{bx}} + (1/\rho_0)\, d_x p = 0. \tag{49}$$

Eqs. (48), (49) describe the frequency domain coupled differential equations. To illustrate the interesting wave dynamics of the phenomena under time-modulated resonant media, let us consider the simple case of an uniform motion: $w_{\mathrm{bx}}(x) = w_{\mathrm{bx}}$, [a simplistic example which is considered here only for the purpose of demonstration (realistic systems would always involve more complex non-uniformed distributions of velocity)]. The wave equation of pressure p is:

$$d_x^2 p - \left[j2\omega w_{\mathrm{bx}}/\left(c^2 - w_{\mathrm{bx}}^2\right)\right] d_x p + \left[\omega^2/\left(c^2 - w_{\mathrm{bx}}^2\right)\right] p = 0. \tag{50}$$

Eq. (50) is a space oscillator with an imaginary term stemming from the convective derivative. Due to space invariance and linearity, we seek for solutions of the form: $p(x) = e^{\xi x}$. Plugging this form of sound pressure into Eq. (50) gives us:

$$\xi = \frac{j\omega(w_{\mathrm{bx}} \pm c)}{c^2\left(1 - \frac{w_{\mathrm{bx}}^2}{c^2}\right)}. \tag{51}$$

ξ corresponds to the effective wave number of the propagating sound. Notice that the imaginary damping coefficient results to neither an attenuated nor parametrically amplified field; an evident remark because we neglected any material losses and the disturbance has a constant uniform velocity, which does not change the system's inertness. It is well known for the stationary case that a resonant frequency for the case of a one-dimensional slab occurs when $L = n\lambda/2$, where $n \in \mathbb{Z}$, L is the length of the slab and λ is the wave length. For the same geometry if we apply a background time modulation of w_{b} the resonant frequency is redshifted (see Appendix):

$$f'_m = \left(1 - \frac{w_{\mathrm{b}}^2}{c^2}\right) f_m. \tag{52}$$

The relation of Eq. (52) is valid for a background movement slower than the speed of sound in the medium, as shown in the Appendix. For the case of $c \le w_{\mathrm{b}}$, the relative speed of the wave as perceived in the stationary observation frame does not allow multiple scattering at the interfaces of the slab, hence the system can no longer be characterized as resonant. To illustrate this remark better, imagine a traveler running in a moving walkway of an airport (as shown in Fig. 2). The speed of the traveler (without the assistance of the walkway) is c, whereas the speed of the walkway floor is w_{b}. The overall speed of the traveler as observed in the stationary frame is $\vec{w}_{\mathrm{b}} + \vec{c}$. In the case, that c is in the same direction with w_{b} [as depicted in Fig. 2(a)] the total speed of the traveler increases in the direction of his choice ($c + w_{\mathrm{b}}$). In the case, that c is in the opposite direction with w_{b} [as depicted in Fig. 2(b)] the total speed is $|w_{\mathrm{b}} - c|$ in the direction of the most dominant velocity c or w_{b}. In order to have a resonant system the "traveler" (whose identity symbolizes the traveling waves inside the slab) should have the ability to run back and forth the walkway so that standing waves can be composed. When $c \le w_{\mathrm{b}}$ the "traveler" has no other option than to head into the direction of the walkway floor (or stay still for $c = w_{\mathrm{b}}$), despite his/her efforts to arrive at the other direction. Of course, for this mathematical analysis of temporal acoustic resonators a smaller velocity disturbance w_{b} with respect to the speed velocity of the medium c is considered.

5. CMT vs. analytical and numerical examples

CMT is an approximate method for the solution of the resonant transmission problem, because it is based on considering only one mode, and it approximates a second-order solution with one of the first order via the slowly varying envelope analysis (similar mathematical analysis can be found when studying soliton solutions in optical fibers). Therefore, we check in this section the validity of the approximate method around the resonant frequency by direct comparison to an analytical and a numerical example. Let us consider the problem of reflection and transmission of a water slab amid air. Water has speed velocity $c = 1498$ m/s and density $\rho_0 = 1000$ kg/m^3, whereas air has $c = 343$ m/s and $\rho_0 = 1.225$ kg/m^3. Assume the background speed of water is zero to the incident wave vector. The slab has a length of $L = 0.2$ m. Such scattering problem can be solved analytically, by considering plane waves and boundary conditions at the boundaries of the water slab and the Sommerfeld radiation conditions at infinity [25]. The obtained analytical solutions

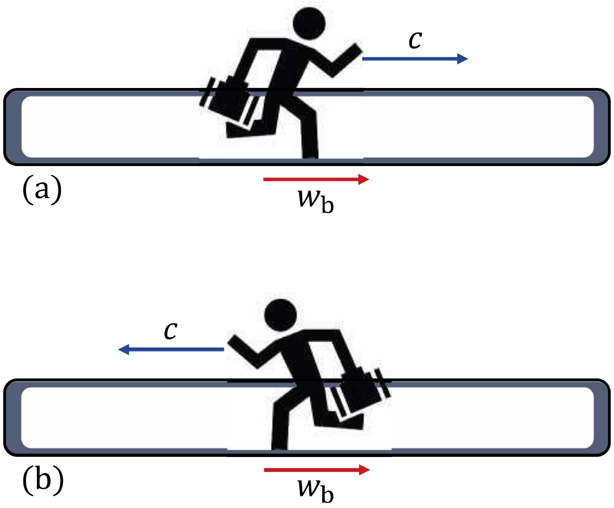

Fig. 2. Traveler running in a moving walkway of an airport, (a) in the same direction as the assisting floor of the walkway, (b) in the opposite direction of the assisting floor of the walkway. If $w_b < c$, the traveler is able to run back and forth between the two sides of the walkway, whereas if $w_b \geq c$ the traveler is heading to the direction of the moving walkway even if he/she chooses to run the opposite direction, or remains still for $w_b = c$. By analogy, a resonator subject to a background medium faster than the sound speed cannot support multiple reflections and the resonance disappears.

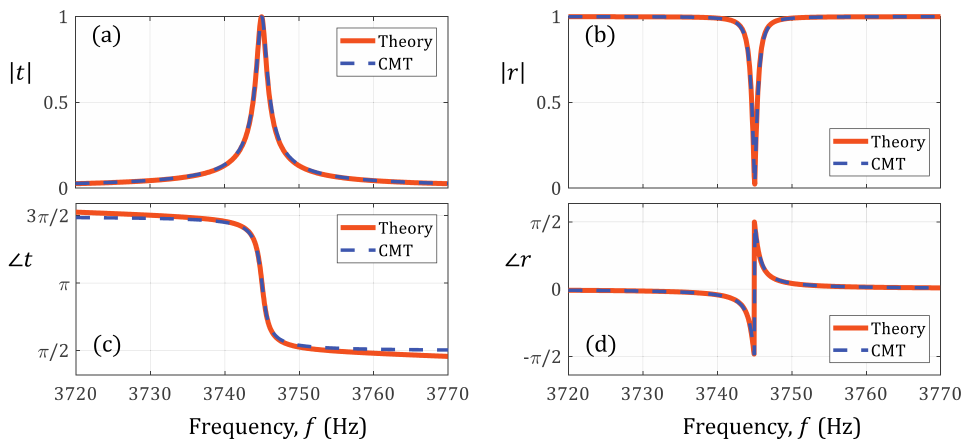

Fig. 3. Numerical example of a 20 cm-thick water slab amid air. (a) Graphical plot and comparison of theory and CMT of the transmission amplitude, (b) graphical plot and comparison of theory and CMT of the reflection amplitude, (c) graphical plot and comparison of theory and CMT of the transmission phase and (d) graphical plot and comparison of theory and CMT of the reflection phase of the wave propagation problem under examination.

match perfectly the prediction obtained from coupled-mode theory. As depicted in Fig. 3(a) and (b) the resonant frequency is $f_m = 3745$ Hz, corresponding to a resonant mode occurring under the condition: $L = \lambda/2$. The dominant mode is odd, hence the transmission has a π phase as explained in Section 3.3 and seen in the phase diagrams [Fig. 3(c), (d)]. The conservation of energy stands, i.e. $|r|^2 + |t|^2 = 1$, where r is the reflection coefficient and t is the transmission coefficient. Furthermore, we obtain the typical Lorentzian shape-line consistent with the prediction of CMT as derived in Section 3.3.

Now let us consider the nonstationary problem of the same geometry, for a background longitudinal disturbance w_b, which we assume relatively smaller than the speed velocity of waves inside water. From the mathematical analysis of Section 5, we expect a redshift of resonant frequency regardless the direction of the disturbance (i.e. independent of whether the wave is in the same or opposite direction of the incident wave). In order to solve such numerical problem, we employ the finite element method (FEM) using modified COMSOL Multiphysics simulations [17] to solve the Eqs. (35) and (36) in the frequency domain and we compare with the solutions obtained by CMT. Our results are depicted in Fig. 4. Fig. 4(a) shows the transmission and Fig. 4(b) shows the reflection from the nonstationary water slab. We considered the stationary state and the cases $w_\mathrm{b} = \pm 0.02c$, $w_\mathrm{b} = \pm 0.03c$ and $w_\mathrm{b} = \pm 0.05c$. As we can see, the results of FEM are in complete agreement with the results acquired by CMT, which are obtained without any fitting parameter. The resonant frequency shifts corroborate the accuracy of the formula in Eq. (52). Of course, the expected Lorentzian shape-lines are

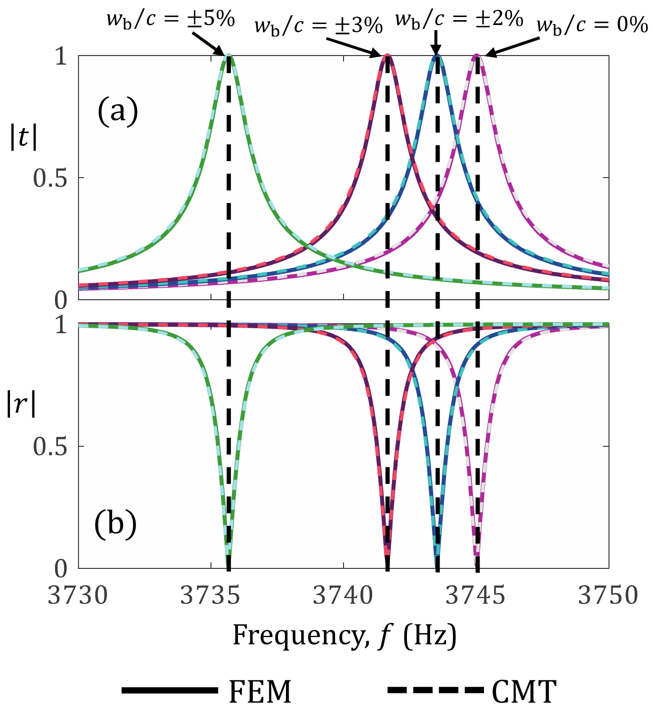

Fig. 4. Graphical plots of FEM and CMT results of nonstationary sound resonators for: $w_b = 0$, $w_b = \pm 0.02c$, $w_b = \pm 0.03c$ and $w_b = \pm 0.05c$, where c is the speed of sound in the slab. Panel (a) portrays the transmission coefficient and (b) the reflection coefficient. Full-wave simulations and CMT agree perfectly without using any fitting parameter.

also found for these cases. We can also verify that conservation of energy is also maintained because we do not consider losses and the constant uniform velocity disturbance does not alter the inertia of the overall resonant system, as explained in Section 4.2.

6. Conclusion

In this work, we developed a simple mathematical approach based on Hamiltonian physics in order to derive analytical formulas for the CMT parameters for the case of two-port scattering through an isolated on-channel resonance. CMT can be utilized and is easily implemented for the solution of general problems regarding sound resonant systems and acoustic wave propagation through reflections and transmission by resonant scattering objects. Notice that although only the one-dimensional example is used in this paper, 2D or 3D ones with oblique incidence can be readily employed by considering the boundary conditions and the effects of material discontinuities for the proper field components. The developed theory of the manuscript can be applied directly to resonant systems of two- or three-dimensions, providing it can be mathematically modeled by a two-port Hermitian system. The advantages of the CMT are two fold: (i) one has to fully solve the eigenvalue problem, including the scattering part, but only for one frequency, i.e. the resonance frequency of the system. Then, the scattering response of the system at any other frequencies around the resonant can be deduced from CMT. (ii) After that, CMT can be used as an orthogonal basis for implementing the perturbation theory and solve a more complicated problem. Such analysis can be utilized to mathematically model the interactions of time-periodically modulated sound resonators or even nonlinear wave properties in acoustical propagation. In order to illustrate the general applicability of coupled-mode theory, we developed the perturbation analysis of the Hamiltonian to deal with a simple didactic example of nonstationary acoustic resonators. We showed that in nonstationary resonant sound systems a uniform background velocity disturbance could alter the eigenfrequencies of the resonator, resulting to a redshifted eigenfrequency response. Numerical simulations employing finite element method to the background moving acoustic medium equations validate our results.

Acknowledgment

This research was supported by the Swiss National Science Foundation (SNSF) under Grant No. 172487.

Appendix. Nonstationary eigenfrequency analysis

Taking into account Eq. (51), we get:

$$\xi = \frac{j\omega(w_{\mathrm{bx}} \pm c)}{c^2\left(1-\frac{w_{\mathrm{bx}}^2}{c^2}\right)} = j\delta \pm j\beta \tag{53}$$

Let us remind that the two solutions of ξ correspond to wave propagation at $-\hat{x}$ and $+\hat{x}$ direction and are valid for any relation between the speed of sound c and the background medium movement velocity w_{bx}. Since we study sound cavities that resonate caused by multiple scattering at the interfaces, the constant part of the wave number $j\delta$ is eliminated due to phase compensation. In more detail for the 1-D sound resonator of length L the phase deviation due to $j\delta$ of the traveling wave at the $+\hat{x}$ direction results: $\phi_\delta^+ = -\delta L$, whereas at the $-\hat{x}$ direction results: $\phi_\delta^- = \delta L$. It is clear that $\phi_\delta^{\mathrm{tot}} = \phi_\delta^+ + \phi_\delta^- = 0$. For this reason, we can easily determine the effective speed velocity (in regards to the computation of the resonant frequency). This expected value is given by the relation:

$$\beta = \frac{\omega}{c\left(1-\frac{w_{\mathrm{bx}}^2}{c^2}\right)} = \frac{\omega}{c_{\mathrm{eff}}}, \tag{54}$$

where $c_{\mathrm{eff}} = c\left(1-\frac{w_{\mathrm{bx}}^2}{c^2}\right)$. The consistent relations for the resonant frequencies for the stationary and nonstationary acoustic problem of the same geometry are:

$$c = \lambda f_m, \tag{55}$$

$$c_{\mathrm{eff}} = \lambda_{\mathrm{eff}} f'_m, \tag{56}$$

and on top of Eqs. (55), (56) we know that $\lambda = \lambda_{\mathrm{eff}} = 2L/n$, where $n \in \mathbb{Z}$ for the one-dimensional sound resonator of a length of L, since they correspond to the resonance response of the one-dimensional sound system (similar conditions can be found for 2-D and 3-D resonators). Dividing Eqs. (55) and (56) we get the relation used directly in Eq. (52) in the main text:

$$f'_m = \frac{c_{\mathrm{eff}}}{c} f_m = \left(1-\frac{w_{\mathrm{bx}}^2}{c^2}\right) f_m. \tag{57}$$

References

[1] A. Yariv, Quantum Electronics, third ed., John Wiley and Sons, 1989.
[2] J.D. Joannopoulos, S.G. Johnson, J.N. Winn, R.D. Meade, Photonic Crystals: Molding the Flow of Light, second ed., Princeton University Press, 2008.
[3] P. Graczyk, M. Krawczyk, Coupled-mode theory for the interaction between acoustic waves and spin waves in magnonic-phononic crystals: Propagating magnetoelastic waves, Phys. Rev. B 96 (2017) 024407.
[4] W.-P. Huang, Coupled-mode theory for optical waveguides: an overview, J. Opt. Soc. Amer. A 11 (1994) 963–983.
[5] H.A. Haus, W. Huang, Coupled-mode theory, Proc. IEEE 79 (1991) 1505–1518.
[6] H. Kogelnik, C.V. Shank, Coupled-wave theory of distributed feedback lasers, J. Appl. Phys. 43 (1972) 2327–2335.
[7] D.N. Maksimov, A.F. Sadreev, A.A. Lyapina, A.S. Pilipchuk, Coupled mode theory for acoustic resonators, Wave Motion 56 (2015) 52–66.
[8] R.F. Pannatoni, Coupled mode theory for irregular acoustic waveguides with loss, Acoust. Phys. 57 (2011) 36–50.
[9] E. Anemogiannis, E.N. Glytsis, T.K. Gaylord, Transmission characteristics of long-period fiber gratings having arbitrary azimuthal/radial refractive index variations, J. Lightwave Technol. 21 (2003) 218–227.
[10] T. Huang, K.H. Wagner, Coupled mode analysis of polarization volume hologram, IEEE J. Quantum Electron. 31 (1995) 372–390.
[11] A. Theocharidis, T. Kamalakis, T. Sphicopoulos, Accuracy of coupled-mode theory and mode-matching method in the analysis of photonic crystal waveguide perturbations, J. Lightwave Technol. 25 (2007) 3193–3201.
[12] T.T. Koutserimpas, R. Fleury, Nonreciprocal gain in non-Hermitian time-floquet systems, Phys. Rev. Lett. 120 (2018) 087401.
[13] T.T. Koutserimpas, R. Fleury, Zero refractive index in time-Floquet acoustic metamaterials, J. Appl. Phys. 123 (2018) 091709.
[14] T. Christopoulos, O. Tsilipakos, N. Grivas, E.E. Kriezis, Coupled-mode-theory framework for nonlinear resonators comprising graphene, Phys. Rev. E 94 (2016) 062219.
[15] V. Grigoriev, F. Biancalana, Coupled-mode theory for on-channel nonlinear microcavities, J. Opt. Soc. Amer. B 28 (2011) 2165–2173.
[16] R.E. Hamam, M. Ibanescu, E.J. Reed, P. Bermel, S.G. Johnson, E. Ippen, J.D. Joannopoulos, M. Soljacic, Purcell effect in nonlinear photonic structures: A coupled mode theory analysis, Opt. Express 16 (2008) 12523–12537.
[17] Comsol multiphysics.
[18] C.F. Sieck, A. Alù, M.R. Haberman, Origins of Willis coupling and acoustic bianisotropy in acoustic metamaterials through source-driven homogenization, Phys. Rev. B 96 (2017) 104303.
[19] M.B. Muhlestein, C.F. Sieck, P.S. Wilson, M.R. Haberman, Experimental evidence of Willis coupling in a one-dimensional effective material element, Nature Commun. 8 (2017) 15625.
[20] Kittel Charles, Introduction to Solid State Physics, Wiley, 1992.

[21] R. Fleury, D.L. Sounas, C.F. Sieck, M.R. Haberman, A. Alù, Sound isolation and giant linear nonreciprocity in a compact acoustic circulator, Science 343 (2014) 516–519.
[22] F. Zangeneh Nejad, R. Fleury, Doppler-based acoustic gyrator, Appl. Sci. 8 (2018) 1083.
[23] G. Galilei, S. Drake, Dialogue Concerning the Two Chief World Systems, Ptolemaic and Copernican, Modern Library, 2001.
[24] V.E. Ostashev, D.K. Wilson, L. Liu, D.F. Aldridge, N.P. Symons, D. Marlin, Equations for finite-difference, time-domain simulation of sound propagation in moving inhomogeneous media and numerical implementation, J. Acoust. Soc. Am. 117 (2005) 503–517.
[25] J. Lekner, Theory of Reflection: Reflection and Transmission of Electromagnetic, Particle and Acoustic Waves, second ed., Springer, 2016.